16.2: Fabrication and Performance Characteristics of Optical Fiber Gratings for Sensing Applications

Youngjoo Chung
Dept. of Info. and Comm.
Kwangju Institute of Science and Technology
Kwnagju 500-712, Korea
ychung@kjist.ac.kr

Un-Chul Paek
Dept. of Info. and Comm.
Kwangju Institute of Science and Technology
Kwnagju 500-712, Korea
ucpaek@kjist.ac.kr

Abstract

Optical fiber gratings, often classified as short-period and long-period fiber gratings according to the magnitude of the period of refractive index modulation along the propagation axis, are increasingly becoming essential components in optical fiber sensors. In this paper, we will discuss fabrication techniques and various performance characteristics of the optical fiber gratings employed in the sensor head. Optical fiber gratings can be fabricated using UV lasers based on the photosensitivity effect, CO_2 laser or electric arc to induce surface deformation and/or stress relaxation, etc. Change of the spectral characteristics of short-period fiber gratings occurs mainly due to variation of the sub-mm grating period. Peak wavelength shift due to environmental change and chirp-induced effects like dual peak separation can be effectively utilized for sensing applications. We will also discuss control of the temperature sensitivity, dual peak separation, and reduction of the polarization-dependent loss (PDL) of long-period fiber gratings and their application to sensing of various physical quantities.

Keywords

Optical fiber sensor, optical fiber grating, temperature sensitivity, resonance peak shift, dual peak separation, polarization-dependent loss (PDL), cascaded long-period fiber grating, phase-shifted long-period fiber grating, sinusoidal chirp

I. INTRODUCTION

Optical fiber gratings have periodic or almost-periodic modulation of the refractive index along the propagation axis and the spectrally selective nature of fiber gratings makes them suitable for applications to various kinds of sensing like strain/temperature sensors, curvature sensors, and load sensors [1-5] as well as fiber-based devices for wavelength division multiplexing (WDM) communications. The index modulation period of short-period fiber gratings, or fiber Bragg gratings (FBGs), is in the sub-*m*m range, while the period of long-period fiber gratings (LPFGs) is of the order of 50 to 500 *m*m.

The fiber Bragg gratings couple the forward and backward propagating core modes and exhibit strong reflection when the resonance condition

$$l_p = 2n\Lambda \tag{1}$$

is satisfied. n is the effective index of the core mode. The long-period gratings, on the other hand, couple the co-propagating core mode and multiple cladding modes and the optical power in the core mode is coupled to the cladding modes at the wavelengths that satisfy the resonance condition

$$l_p = \left(n_{co} - n_{cl}^{(m)}\right)\Lambda \tag{2}$$

and eventually leaks out through the cladding region. n_{co} and $n_{cl}^{(m)}$ are the effective indexes of the core mode and the m-th cladding mode, respectively.

The effective index of a fiber mode has a complex dependence on the refractive index profile and the constituent materials of the fiber, and the external environment can have a considerable effect on the spectral characteristics. The grating period Λ can also vary due to the environmental effect. These combined effects make the spectral characteristics of optical fiber gratings sensitive to changes in the environment, e.g., temperature, strain, pressure, and ambient index. The optical fiber sensors that utilize such characteristics offer important advantages such as low insertion loss, high wavelength selectivity, high sensitivity, EMI immunity, and multiplexing capabilities.

The measurement sensitivity of optical fiber grating-based sensors can be enhanced by cascading multiple LPFGs in series. In single-mode fibers, an LPFG couples the fundamental HE_{11} core mode and multiple forward-propagating HE_{1m} cladding modes and thus have higher sensitivity to the external perturbation than FBGs. One drawback of LPFGs, however, is the relatively large rejection bandwidth, which may reduce the measurement resolution. Cascaded LPFGs with proper separation between gratings exhibit fine interference fringes in the transmission spectrum, which can be utilized to significantly enhance the resolution. These have been used as fiber-based WDM filters [6] and temperature sensing elements [7].

In this paper, we will discuss the fabrication techniques and various performance characteristics of the optical fiber gratings employed in the sensor head. The rest of this paper will be organized as follows. In Section II, we will briefly review

the principles of calculating the spectral characteristics of optical fiber gratings based on the coupled-mode theory and the transfer matrix. The fabrication techniques for the optical fiber gratings will then be discussed in Section III, and application of optical fiber gratings to sensing of various physical quantities like temperature, bending, transverse load, and ambient index will be discussed in Section IV. This paper will conclude with a summary in Section V.

II. SPECTRAL CHARACTERISTICS

The spectral characteristics of optical fiber gratings with a given specification of the refractive index modulation can be modeled using the coupled mode theory [8-10] and the method of transfer matrix. The coupled modes are the counter-propagating core modes in FBGs and co-propagating core and cladding modes in LPFGs. The inverse process of obtaining the grating structure from a given specification of the spectrum can be also done using a variety of approaches [12-14].

For example, in case of the FBG, the forward- and backward-propagating modes obey the coupled-mode equations expressed as [8]

$$\begin{aligned} \frac{dA_f}{dz} &= ik\, e^{-if} e^{i\Delta b\, z} A_b, \\ \frac{dA_b}{dz} &= -ik\, e^{if} e^{-i\Delta b\, z} A_f, \end{aligned} \tag{3}$$

where A_f and A_b are the slowly varying envelope functions for the forward- and backward-propagating modes, respectively, and k and f are the magnitude and phase of the coupling coefficient. The detuning parameter Δb is given by

$$\Delta b = 2b_{co} - \frac{2p}{\Lambda} = 2p\left(\frac{2n}{l} - \frac{1}{\Lambda}\right), \tag{4}$$

where n is the effective index of the core mode, and Λ is the grating period.

Equation (3) yields the solution in analytic form for a uniform grating with constant grating parameters k, f, and Λ. The amplitudes of the modes at the output end of the grating are related to those at the input end through the transfer matrix $\mathbf{F}(L)$ [11,15,16] as

$$\begin{pmatrix} A_f(L) \\ A_b(L) \end{pmatrix} = \mathbf{F}(L) \cdot \begin{pmatrix} A_f(0) \\ A_b(0) \end{pmatrix}, \tag{5}$$

where

$$\mathbf{F}(L) = \begin{pmatrix} e^{-i\Delta bL/2}\left(\cosh sL + i\frac{\Delta b}{2s}\sinh sL\right) & i\frac{k e^{-if} e^{+i\Delta bL/2}}{s}\sinh sL \\ -i\frac{k e^{if} e^{i\Delta bL/2}}{s}\sinh sL & e^{i\Delta bL/2}\left(\cosh sL - i\frac{\Delta b}{2s}\sinh sL\right) \end{pmatrix}, \tag{6}$$

and $s = \sqrt{k^2 - \Delta b^2/4}$.

The grating parameters k, f, and Λ can vary along the axial direction z for non-uniform gratings. For numerical simulation, the grating length is subdivided into a number of sections, within each of which the grating parameters are constant. The full transfer matrix of the grating is then obtained as the product of the constituent transfer matrices. The transmission spectrum is then obtained by setting $A_f(0) = 1$ and $A_b(L) = 0$. Figure 1 shows the transmission spectrum of an apodized FBG under varying external strain. The strain sensitivity of the peak wavelength shift is approximately 3.7 nm/%ε.

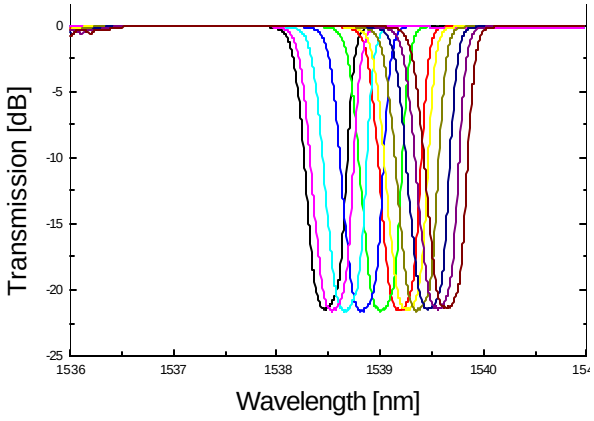

Fig. 1: Shift of the resonance wavelength for FBG under varying external strain.

Spectral characteristics of the LPFG can be analyzed in a similar manner. Figure 2 shows the transmission spectrum of a cascaded LPFG with 95 cm separation between a pair of LPFGs. The overall envelope bandwidth is about 60 nm and the channel spacing is 0.56 nm.

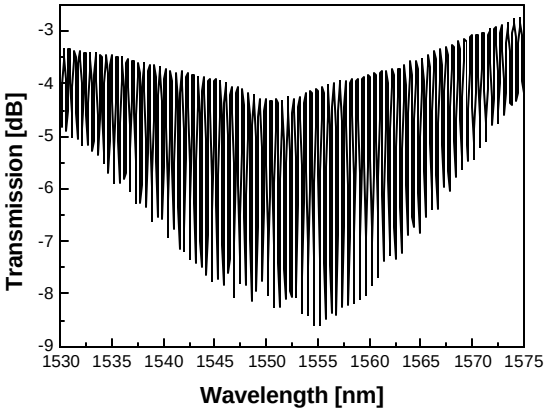

Fig. 2: Measured transmission spectrum of cascaded LPFGs.

III. FABRICATION OF OPTICAL FIBER GRATINGS

FBGs are fabricated typically using UV lasers based on the photosensitivity effect [17-19]. Excimer lasers with low coherence are used with phase masks to produce UV laser

intensity modulation. Argon-ion lasers have long coherence and are suitable for interferometric method in which the two split UV beams intersect with each other at the location of the photosensitive optical fiber [20].

LPFGs are usually fabricated with the amplitude mask method or the point-by-point method. The refractive index change can be induced by using UV laser, CO_2 laser or electric arc. Based on these methods, several techniques have been developed for fabrication of the LPFGs: (1) irradiation of UV laser beam on hydrogen-loaded GeO_2-doped fibers [21] with the photosensitivity effect; (2) periodic relaxation of residual stress with a CO_2 laser [22,23]; (3) periodic physical deformation of the core with electric arc or CO_2 laser [24]; (4) microbending with electric arc [25] (5) thermal diffusion in nitrogen-doped silica-core fiber with electric arc or CO_2 laser [26].

Azimuthally Symmetric LPFG

The polarization-dependent loss (PDL) of the LPFGs can be significantly reduced by exposing the fiber to the writing beam in a symmetric manner [27]. In this case, the method for fabrication of LPFGs was based on the point-by-point method using a CO_2 laser that induces surface deformation on the optical fiber.

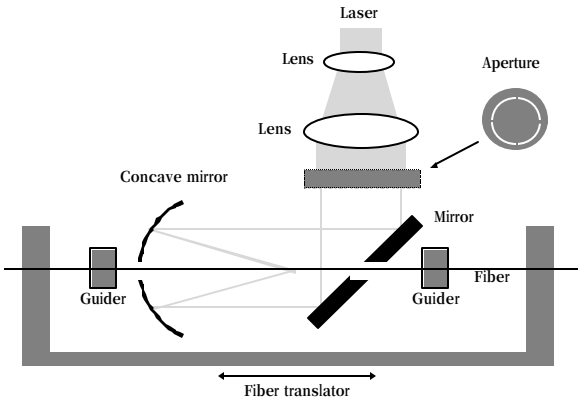

Fig. 3: Setup for fabricating azimuthally symmetric LPFG.

In the fabrication setup designed to induce azimuthally symmetric refractive index changes (see Fig. 3), the CW CO_2 laser beam is first expanded by approximately 8 times by a pair of convex lenses. The expanded beam is then passed through an annular spatial filter to form a ring-shaped beam. This increases the focal spot size and helps alleviate the alignment difficulty. The annular laser beam is then deflected by a flat mirror tilted at 45° into the axial direction of the fiber and is focused on the fiber by a concave mirror with the focal length of 50 mm for symmetric exposure. These two mirrors have holes at the center for the optical fiber to pass through.

The optical fiber is suspended horizontally and supported by two guiders located close to the mirrors for precise alignment as required for symmetric laser beam exposure. The mirrors and guiders are fixed and the fiber is translated in the axial direction across the guiders while clamped on the translation stage. The LPFG is fabricated as the translation stage is moved at predetermined intervals in synchronization with the CO_2 laser beam exposure using the point-by-point method.

The maximum measured PDL was 1.85 dB at 1534 nm for the conventional single-side exposure case and 0.21 dB at 1506 nm for the symmetric exposure case. In comparison, the standard single-mode fiber showed 0.17 dB of PDL on the average with the 0.07 dB noise level. The PDL of the measurement system itself, e.g., the polarization dependence of the detector, was not considered in the analysis. This result indicates that the LPFG fabricated with the symmetric exposure method has the PDL that is quite comparable to that of the standard single-mode fiber.

IV. APPLICATIONS TO OPTICAL FIBER SENSING

Temperature Sensitivity

The effective index of a fiber mode has a complex dependence on the refractive index profile and the constituent materials of the fiber. Change of the mechanical and material properties of the fiber and consequent change in the response of the fiber grating is a typical problem that needs to be addressed for successful implementation of fiber grating-based sensors.

Temperature and strain discrimination of fiber grating-based sensors can be done in a variety of ways. H. J. Patrick *et al.* [28] presented a sensor head with combination of two fiber Bragg gratings and a long-period fiber grating. Other approaches based on material properties were also proposed, e.g., germanosilicate and boron-codoped germanosilicate fibers [29] and single-mode fiber and Er/Yb-codoped fiber [30], where different fibers were spliced and fiber Bragg gratings were fabricated on the joint region such that different sensitivities to temperature but similar sensitivities to strain could be obtained. Another sensor design using two superimposed fiber gratings with different resonance wavelengths to obtain different strain and temperature sensitivities was proposed [31], and other types of sensor heads based on spliced fibers with different diameters [32] and a fiber etalon and a fiber Bragg grating [33] were demonstrated.

Several methods have been proposed to minimize the temperature sensitivity of LPFG [34-36]. Among them, the GeO_2-B_2O_3 co-doped core fiber [35] is of particular interest since it is based on a simple step index structure with the matched cladding without resorting to elaborate waveguide design. Utilizing the opposite signs of the thermo-optic coefficients of GeO_2 and B_2O_3 referenced to SiO_2, the effective thermo-optic coefficient of the core could be adjusted to match that of the silica cladding.

With the optimized doping concentrations of GeO_2 and B_2O_3, the temperature sensitivity was suppressed to as low as 0.002 nm/°C [37]. The strain sensitivity of the same fiber was measured to be 0.42 pm/*m*strain. The measurement results for the resonance wavelength shift in LPFG with temperature and strain changes are shown in Fig. 4. The extremely low temperature sensitivity makes this LPFG ideal for strain sensing immune to temperature variation of the environment. The negative temperature sensitivity of the LPFG demonstrates the effect of co-doping B_2O_3 and P_2O_5 in the core. Excessive co-doping overcompensated the positive temperature sensitivity due to GeO_2 and the measured temperature sensitivity was -0.14 nm/°C.

Enhancement of the temperature sensitivity for the purpose of temperature sensing can be achieved by doping the depressed inner cladding of the silica-core fiber with B_2O_3. The measurement results indicate the enhanced temperature sensitivity of 0.28 nm/°C. The excellent stability at high temperature and low insensitivity to the strain makes the silica-core fiber ideal for temperature sensing [38].

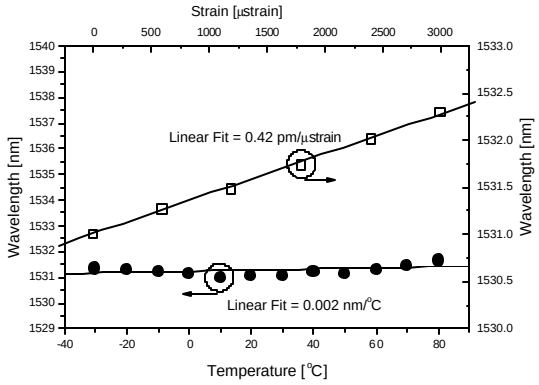

Fig. 4: Temperature dependence of the resonance wavelength of the LPFG with suppressed temperature sensitivity. The linear fits for the temperature and strain have slopes of +0.002 nm/°C and 0.42 pm/*m*strain, respectively.

Resonance Peak Shift and Splitting in LPFG

Exposing the LPFG region directly to a UV laser beam without an amplitude mask has the effect of reducing the photo-induced index modulation (AC component) while increasing the index of the photosensitive region of the fiber (DC component). As a consequence, the coupling strength is reduced and the resonance peak is shifted to the longer wavelength.

Decrease of the coupling constant k with the UV post-exposure can either increase or decrease the peak depth of the LPFG since the transmittivity varies like $\cos^2(kL)$, where L is the grating length. If the LPFG is exposed to the UV beam with the peak depth unsaturated, as manifested by the continued growth of the peak depth during the grating formation, the peak depth will decrease with the UV fluence due to the reduction of the coupling constant. On the other hand, if the peak depth has been saturated and decreases during the grating formation, the peak depth will grow with the UV fluence even though the coupling constant k decreases.

In LPFGs, the phase matching condition is

$$d(l) = \frac{1}{2p}(b_{co} - b_{cl}^{m}) = \frac{1}{l}(n_{co} - n_{cl}^{m}) = \frac{1}{\Lambda}, \qquad (7)$$

where Λ is the grating period, and the resonance peaks appear at the wavelengths that satisfy Eq. (7). A single resonance peak appears for lower-order cladding modes, but dual peaks can appear for high-order cladding modes for which $d(l)$ is not monotonic in certain wavelength range. By shifting $d(l)$ in the upward direction while keeping the grating factor $1/\Lambda$ unchanged using the technique of UV post-exposure, the two resonance peaks can be made to coalesce into a resonance peak of wide bandwidth as large as 200 nm. If the average index decreases due to some perturbation in the cladding region, the two peaks shift in the opposite direction and peak splitting occurs as shown in the inset of Fig. 5. This can be interpreted as that reduction of the index difference causes the resonant peak splitting of LPFGs with the external perturbation change. Such resonant peak splitting with the external perturbation change makes the LPFGs very useful for sensing applications.

Application of the resonance peak splitting to bending curvature sensor is shown in Fig. 5. The polynomial fitting of the peak separation gives [39]:

$$l_{sep}[\text{nm}] = 96.96 + 90.56C - 11.94C^2 \qquad (8)$$

where C is the curvature in the unit of m^{-1}. The resonance peak splitting in LPFG can be applied to other kinds of optical fiber sensors like ambient index and transverse load.

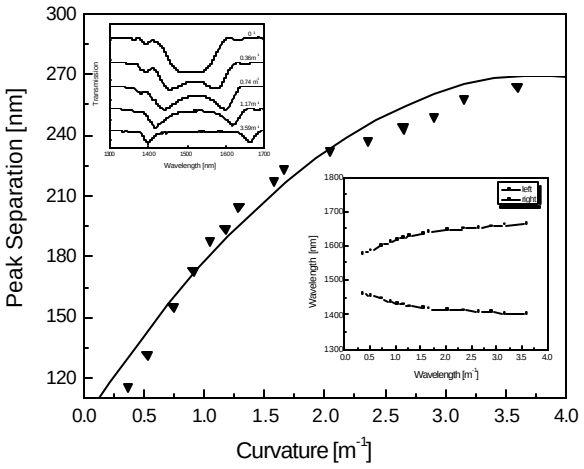

Fig. 5: Dependence of characteristics of LPFGs on bending. Peak splitting occurs as the bending curvature changes.

Cascaded LPFGs

An LPFG pair cascaded in series is characterized by fine interference fringe pattern and narrow bandwidth. Dependence of the resonant wavelength shift and peak depth change of an LPFG pair on external environment change can be utilized for sensing applications, e.g., bending curvature, transverse load, and ambient index [40].

Figure 6 shows the sensitivity of the transmission spectrum of the LPFG pair to the ambient index changes. Shift of the resonant fringe with the ambient index change is shown in the inset. Since the effective indexes and the field profiles of the cladding modes change in response to the ambient index change in the grating-free region, the contrast of the interference fringe pattern is degraded and the peak wavelength shifts occur. If the ambient index is close to that of the effective index of the cladding mode, the interference between the core and cladding modes in the second grating disappears altogether. As the ambient index is further increased, the interference pattern appears again due to the modes that propagate in the surrounding region. Since the transmission characteristics of the LPFG pair heavily depend on the ambient index change, the LPFG pair will be useful as the oil and chemical sensors.

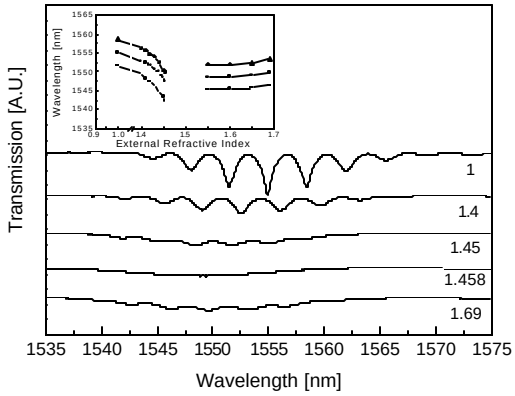

Fig. 6: Changes of the transmission characteristics of an LPFG pair due to the surrounding refractive index change. The resonant fringe shift with the ambient index change is shown in the inset.

Phase-shifted LPFG

The transmission characteristics of LPFGs can be adjusted, e.g. by using the phase-shifted LPFGs [41] whose resonant wavelength and peak depth can be controlled as in the case of tailoring of the EDFA gain-flattening filters [42]. The phase-shift technique has also been used with fiber Bragg gratings (FBGs) for transverse load sensing [43].

The transmission characteristics of the LPFG can be altered by the tension and compression strain induced by the bending curvature. This effect can be used for application of the phase-shifted LPFGs to tunable bandpass filters and sensing of directional bending [44]. Change of the transmission characteristics of the phase-shifted LPFGs depends on the initial coupling strength during the process of fabrication by UV post-exposure on half of the grating region. Since the UV post-exposure increases the effective index of the core mode and thus induces phase shift, the resonant wavelength shifts to the longer wavelength. The coupling strength decreases simultaneously, and the loss peak depth decreases and eventually disappears completely for the first saturated or unsaturated LPFGs, while it disappears and appears again for the second saturated LPFGs. This effect is depicted in Fig. 7 as the increase of the depth of the loss peak beginning near the wavelength of 1510 nm.. Refractive index modulation of second saturated LPFG larger than that of first saturated or unsaturated LPFGs implies that larger phase shift can be induced before the grating structure is erased.

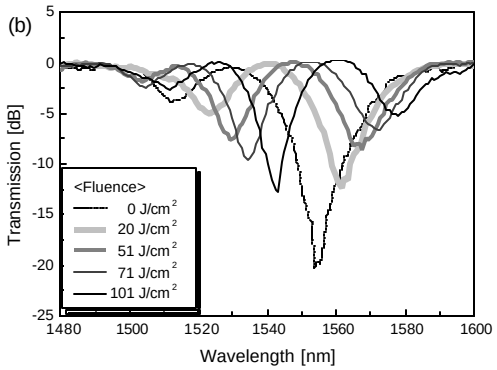

Fig. 7: The transmission spectra of the phase-shifted LPFG fabricated with the second saturated LPFG for different fluence of UV post-exposure.

Sinusoidal Chirp-induced Effects in FBG

FBG-based sensors typically require use optical spectrum analyzers in order to monitor the shift of the resonance Bragg wavelength due to the change of the measurands. Other types of signal demodulators like Mach-Zehnder interferometer (MZI), Fabry-Perot filter, and acousto-optic filter can be used in combination with the fiber Bragg gratings in the sensor system to convert the wavelength-encoded signal into electrical signals to facilitate real-time monitoring [45-47]. These methods, however, do not fully utilizes the advantage of potential for all-optical signal processing provided by the optical fiber. One solution would be to measure the change of intensity rather than the wavelength shift, e.g., using chirped FBGs [46,48]. Chirped FBGs can be made by using chirped phase masks, and other less costly methods employ UV irradiation, heating and bending of conventional FBGs.

Sinusoidal chirp of the grating period can be induced in an originally unchirped FBG by displacing one end of the fiber in the axial direction with the other end fixed [49]. This al-

lows control of the reflection bandwidth by adjusting the amount of axial displacement, and conversely, this effect can be used to sense the displacement or motion of an object by measuring the intensity of the transmitted light [50]. Figure 8 shows the reflection spectra of the FBG for different amount of sinusoidal chirp.

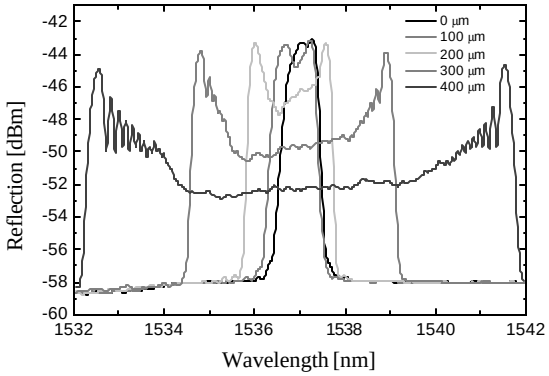

Fig. 8: Change of the reflection spectrum with increase of the displacement and the sinusoidal chirp.

V. SUMMARY

We discussed in this paper the spectral characteristics and fabrication of optical fiber gratings and their application to sensing. The spectral characteristics of the optical fiber gratings are determined by the grating parameters like the amplitude and phase of the index modulation and the grating period. The index profile of the optical fiber and the properties of the modes also play an important role.

There are various methods available for fabrication of the fiber gratings. Short-period fiber gratings, or fiber Bragg gratings (FBGs), are typically fabricated using a UV laser and a phase mask or using the interferometric method. Long-period fiber gratings (LPFGs) can be fabricated using several methods like amplitude mask, periodic relaxation of residual stress, periodic physical deformation of the core, microbending with electric arc, and thermal diffusion in nitrogen-doped silica-core fiber.

We also discussed various principles of optical fiber grating-based sensors such as temperature sensitivity, resonance peak shift and splitting in LPFG, cascaded LPFG, phase-shifted LPFG, and sinusoidal chirp-induced effects in FBGs.

ACKNOWLEDGMENTS

This work was partially supported by KISTEP through Critical Technology 21 Program and by BK-21 Program, MOE, Korea. Thanks go to the current and former graduate students who performed the work described in this paper, especially H. S. Park, Y. G. Han, C. S. Kim, S. T. Oh and J. S. Song.

VI. REFERENCES

[1] V. Bhatia, A. M. Vengsarkar, *Opt. Lett*., vol. 21, no. 9, pp. 692-694, 1996

[2] Y. G. Han, C. S. Kim, K. Oh, U. C. Paek, and Y. Chung, *OFS 13*, Kyongju, Tu2-7, pp. 58-61, 1999

[3] H. J. Patrick and S. T. Vohra, *OFS 13*, Kyongju, pp. 561-564, 1999

[4] H. J. Patrick, C. C. Chang, and S. T. Vohra, *Electron. Lett*., vol. 34, no. 18, pp. 1773-1775, 1998

[5] Y. Liu, L. Zhang, and I. Bennion, *Electron. Lett*., vol. 35, no. 8, pp. 661-663, 1999

[6] X. J. Gu, *Opt. Lett*., vol. 23, no. 7, pp. 509-510, 1998

[7] B. H. Lee and J. Nishii, *OFS 13*, Kyongju, pp. 418-421, 1999

[8] A. Yariv, *IEEE J. Quantum Electron*., vol. QE-9, no. 9, pp. 919-933, 1973

[9] T. Erdogan, *J. Lightwave Technol*., vol. 15, no. 8, pp. 1277-1294, 1997

[10] M. McCall, *J. Lightwave Technol*., vol. 18, no. 2, pp. 236-242, 2000

[11] M. Yamada and K. Sakuda, *Appl. Opt*., vol. 26, no. 16, pp. 3474-3478, 1987

[12] L. Poladian, *Opt. Lett*., vol. 25, no. 11, pp. 787-789, 2000

[13] J. Skaar, L. Wang, and T. Erdogan, *IEEE Photon. Technol. Lett*., vol. 37, no. 2, pp. 165-167, 2001

[14] G. Cormier, R. Boudreau, S. Theriault, *J. Opt. Soc. Am. B*, vol. 18, no. 12, pp. 1771-1776, 2001

[15] W. P. Huang and J. Hong, *J. Lightwave Technol*., vol. 10, no. 10, pp. 1367-1375, 1992

[16] G. W. Chern, and L. A. Wang, *J. Opt. Soc. Am. A*, vol. 16, no. 11, pp. 2675-2689, 1999

[17] K. O. Hill, B. Malo, F. Bilodeau, and D. C. Johnson, *Annu. Rev. Mater. Sci*., vol. 23, pp. 125-157, 1993

[18] D. L. Williams, B. J. Ainslie, J. R. Armitage, R. Kashyap and R. Campbell, *Electron. Lett*., vol. 29, no. 1, pp. 45-47, 1993

[19] T. A. Strasser, T. Erdogan, A. E. White, V. Mizarahi, and P. J. Lemaire, *Appl. Phys. Lett*., vol. 65, pp. 3308-3310, 1994

[20] Y. Wang, J. Grant, A. Sharma, G. Myers, *J. Lightwave Technol*., vol. 19, no. 10, pp. 1569-1573, 2001

[21] A. M. Vengsarkar, P. J. Lemaire, J. B. Judkins, V. Bhatia, T. Erdogan and J. E. Sipe, *J. Lightwave Technol*., vol. 14, no. 1, pp. 58-65, 1996

[22] M. Akiyama, K. Nishide, K. Shima, A. Wada, R. Yamauchi, *OFC 98*, San Jose, ThG1, pp. 276-277, 1998

[23] T. Enomoto, M. Shigehara, S. Ishikawa, T. Danzuka, and H. Kanamori, *OFC 98*, San Jose, ThG2, pp. 277-278, 1998

[24] C. Narayanan, H. M. Presby and A. M. Vengsarkar, *Electron. Lett*., vol. 33, no. 4, pp. 280-281, 1997

[25] I. K. Hwang, S. H. Yun, H. S. Kim, and B. Y. Kim, *OECC 98*, Chiba, 14C1-2, pp. 144-145, 1998

[26] V. I. Karpov, M. V. Grekov, E. M. Dianov, K. M. Golant, S. A. Vasiliev, O. I. Medvedkov, R. R. Khrapko, *OFC 98*, San Jose, ThG4, pp. 279-280, 1998

[27] S. T. Oh, C. I. Song, B. H. Lee, W. T. Han, U. C. Paek, and Y. Chung, *OECC 2001*, Sydney, pp. 22-23, 2001

[28] H. J. Patrick, G. M. Williams, A. D. Kersey, J. R. Pedrazzani, and A. M. Vengsarkar, *IEEE Photon. Technol. Lett*., vol. 8, no. 9, pp. 1223-1225, 1996

[29] P. M. Cavaleiro, F. M. Araujo, L. A. Ferreira, J. L. Santos, and F. Farahi, *IEEE Photon. Technol. Lett*., vol. 11, no. 12, pp. 1635-1637, 1999

[30] B.-O. Guan, H.-Y. Tam, S.-L. Ho, W.-H. Chung and X.-Y. Dong, *Electron. Lett*., vol. 36, no. 12, pp. 1018-1019, 2000

[31] M. G. Xu, J.-L. Archambault, L. Reekie, and J. P. Dakin, *Electron. Lett*., vol. 30, no. 13, pp. 1085-1087, 1994

[32] S. W. James, M. L. Dockney and R. P. Tatam, *Electron. Lett*., vol. 32, no. 12, pp. 1133-1134, 1996

[33] H. Singh, J. Sirkis, *OFS 11*, Sapporo, Tu5-1, pp. 108-111, 1996

[34] J. B. Judkins, J. R. Pedrazzani, D. J. DiGiovanni, and A. M. Vengsarkar, *OFC 96*, PD1, 1996

[35] K. Shima, K. Himeno, T. Sakai, S. Okude, A. Wada, and R. Yamauchi, *OFC 97*, Dallas, FB2, pp. 347-348, 1997

[36] A. A. Abramov, A. Hale, and A. M. Vengsarkar, *OFC 97*, Dallas, PD3, 1997

[37] Y. G. Han, H. S. Park, W. T. Han, B. H. Lee, U. C. Paek, Y. Chung, C. S. Kim, *OFC 2000*, Baltimore, TuB3, pp. 26-28, 2000

[38] D. S. Yamasaki, M. Akiyama, K. Nishide, A. Wada, and R. Yamauchi, *OFS 13*, Kyongju, pp. 385-388, 1999

[39] Y.-G. Han, B. H. Lee, W.-T. Han, U.-C. Paek, and Y. Chung, *OECC 2001*, Sydney, pp. 315-316, 2001

[40] Y.-G. Han, B. H. Lee, W.-T. Han, U.-C. Paek, and Y. Chung, *Meas. Sci. Technol*., vol. 12, no. 7, pp. 778-781, 2001

[41] L. Wei and J. W. Y. Lit, *J. Lightwave Technol*., vol. 15, no. 8, pp. 1405-1410, 1997

[42] J. R. Qian, H. F. Chen, *Electron. Lett*., Vo. 34, no. 11 , pp. 1132 -1133, 1998

[43] M. LeBlanc, S. T. Vohra, T. E. Tsai, E. J. Friebele, *Opt. Lett*., vol. 24, no. 16, pp. 1091- 1093 , 1999

[44] Y.-G. Han, W.-T. Han, U.-C. Paek, and Y. Chung, *OFS 2002*, Portland, TuP5, 2002

[45] M. G. Xu, H. Geiger, J. L. Archambault, L. Reekie and J. P. Dakin, *Electron. Lett*., vol. 29, no. 17, pp. 1510-1511, 1993

[46] S. Kim, S. Kim, J. Kwon, and B. Lee, *IEEE Photon. Technol. Lett*., vol. 13, no. 8, pp. 839-841, 2001

[47] A. D. Kersey, T. A. Berkoff and W. W. Morey, *Electron. Lett*., vol. 28, no. 3, pp. 236-238, 1992

[48] S. Kim, J. Kwon, S. Kim, and B. Lee, *IEEE Photon. Technol. Lett*., vol. 12, pp. 678-680, 2000

[49] E. Suhir, *J. Lightwave Technol*., vol. 14, no. 2, pp. 144-147, 1996

[50] J. Song, H. Park, W.-T. Han, U.-C. Paek, and Y. Chung, *OFS 2002*, Portland, TuP 27, 2002